Reaction Mechanism of *Escherichia coli* Dihydrodipicolinate Synthase Investigated by X-ray Crystallography and NMR Spectroscopy[†,‡]

Stefan Blickling,[*,§] Christian Renner,[§] Bernd Laber,[||] Hans-Dieter Pohlenz,[||] Tad A. Holak,[§] and Robert Huber[§]

Max-Planck-Institut für Biochemie, Abteilung Strukturforschung, Am Klopferspitz 18a, D-82152 Martinsried, FRG, and Hoechst Schering AgrEvo GmbH, Biochemie, Gollanczstrasse 71, D-13465 Berlin, FRG

Received September 10, 1996; Revised Manuscript Received October 25, 1996[⊗]

ABSTRACT: Dihydrodipicolinate synthase (DHDPS) catalyzes the condensation of pyruvate with L-aspartate β-semialdehyde. It is the first enzyme unique to the diaminopimelate pathway of lysine biosynthesis. Here we present the crystal structures of five complexes of *Escherichia coli* DHDPS with substrates, substrate analogs, and inhibitors. These include the complexes of DHDPS with (1) pyruvate, (2) pyruvate and the L-aspartate β-semialdehyde analog succinate β-semialdehyde, (3) the inhibitor α-ketopimelic acid, (4) dipicolinic acid, and (5) the natural feedback inhibitor L-lysine. The kinetics of inhibition were determined, and the binding site of the L-lysine was identified. NMR experiments were conducted in order to elucidate the nature of the product of the reaction catalyzed by DHDPS. By this method, (4*S*)-4-hydroxy-2,3,4,5-tetrahydro-(2*S*)-dipicolinic acid is identified as the only product. A reaction mechanism for DHDPS is proposed, and important features for inhibition are identified.

Dihydrodipicolinate synthase (DHDPS,[1] EC 4.2.1.52) is the first enzyme unique to the lysine biosynthetic pathway of procaryotes, some *Phycomycetes*, and higher plants. It catalyzes the condensation of pyruvate and L-aspartate β-semialdehyde (L-ASA) (Yugari & Gilvarg , 1965). On the basis of indirect evidence, it has been suggested that the product released by DHDPS is L-2,3-dihydrodipicolinic acid (2,3-DHDP), which is then converted by dihydrodipicolinate reductase to L-2,3,4,5-tetrahydrodipicolinic acid (THDP) (Figure 1).

DHDPS has been isolated from a variety of bacterial (Shedlarski & Gilvarg, 1969; Stahly, 1969; Cremer *et al.*, 1988) and plant (Frisch *et al.*, 1991; Ghislain *et al.*, 1990; Kumpaisal *et al.*, 1987) sources. In all cases examined, the reaction proceeds *via* a ping-pong mechanism in which pyruvate binds as a Schiff base to the ϵ-amino group of a lysine residue in the active site of the enzyme. Then, L-ASA binds to the active site, and the product is released. The details of the reaction however remained unclear. According to the classification of Grazi *et al.* (1962), DHDPS is a type I aldolase.

Depending on their regulatory properties, DHDPS enzymes can be grouped into three classes: plant enzymes which are strongly inhibited by lysine with an $I_{0.5}$ between 0.01 and 0.05 mM (Frisch *et al.*, 1991; Ghislain *et al.*, 1990; Dereppe *et al.*, 1992; Wallsgrove & Mazelis, 1981; Kumpaisal *et al.*, 1987), enzymes from *Escherichia coli*, *Bacillus sphaericus*, and *Methanobacterium thermoautotrophicum* which are only weakly inhibited with an $I_{0.5}$ between 0.25 and 1.0 mM (Laber *et al.*, 1992; Barlett & White, 1986; Bakhiet *et al.*, 1984), and DHDPS from most Gram-positive bacteria which appear not to be inhibited by lysine at all ($I_{0.5}$ > 10 mM; Selli *et al.*, 1994; Webster & Lechowitch, 1970; Stahly, 1969; Cremer *et al.*, 1988; Hoganson & Stahly, 1975; Yakamura *et al.*, 1974; Tosaka & Takinami, 1978). The molecular mechanism by which lysine exerts its regulatory effect in sensitive enzymes is still a matter of controversy. Lysine has been shown to inhibit wheat DHDPS competitively with respect to L-ASA, suggesting an overlap of the lysine and ASA binding sites (Kumpaisal *et al.*, 1987); inhibition of the maize enzyme is reported to be competitive with respect to pyruvate (Frisch *et al.*, 1991), indicative of an overlap of the lysine and pyruvate binding sites, although recent mutagenesis studies by the same group support the view that lysine acts as an allosteric inhibitor (Shaver *et al.*, 1996).

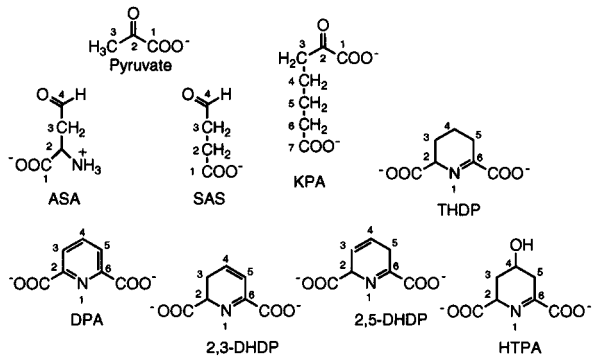

FIGURE 1: Formulas of compounds mentioned in the text.

The crystal structure of *E. coli* DHDPS has recently been solved at a resolution of 2.5 Å by X-ray crystallography (Mirwaldt *et al.*, 1995). The quarternary structure of this homotetrameric enzyme is best described as a dimer of dimers, with weak contacts between the two dimers compared to the intradimer contacts. The monomer has a

[†] This work was supported by DFG-SFB 266 (T.A.H.).

[‡] Coordinates of *E. coli* DHDPS have been deposited in the Brookhaven Protein Data Bank (Tracking Number T8136).

* To whom correspondence should be addressed. Telephone: 0049 89 8578 2661. Fax: 0049 89 8578 3516. E-mail: blicklin@biochem.mpg.de.

[§] Max-Planck-Institut für Biochemie.

[||] Hoechst Schering AgrEvo GmbH.

[⊗] Abstract published in *Advance ACS Abstracts,* December 1, 1996.

[1] Abbreviations: ASA, aspartate β-semialdehyde; 2,3-DHDP, L-2,3-dihydrodipicolinic acid; 2,5-DHDP, L-2,5-dihydrodipicolinic acid; DHDPS, dihydrodipicolinic acid synthase; DPA, dipicolinic acid; HTPA, (4S)-4-hydroxy-2,3,4,5-tetrahydro-(2*S*)-dipicolinic acid; KPA, α-ketopimelic acid; Neu5Ac, *N*-acetylneuraminate lyase; SAS, succinate β-semialdehyde; THDP, L-2,3,4,5-tetrahydrodipicolinic acid.

S0006-2960(96)02272-6 CCC: $14.00 © 1997 American Chemical Society

Table 1: Crystallization and Soaking Conditions

	buffer	additions	soaking time
native[a]	1.8 M potassium phosphate (pH 10)	1 μL of 6% β-octyl glucoside to drop	
derivatives			
KPA	2.3 M potassium phosphate (pH 10)	50 mM KPA	3 h
LPS	2.0 M potassium citrate (pH 5.7)	40 mM pyruvate/120 mM SAS/80 mM lysine	4 days
LYS	2.3 M potassium phosphate (pH 10.0)	100 mM lysine	5 days
PHP	2.3 M potassium phosphate (pH 10.0)	50 mM pyruvate/50 mM hxdroxyproline	1 day
DIP		cocrystallization of DHDPS with 50 mM DPA under native conditions	

[a] After 2−3 days, crystals (0.8 mm × 0.8 mm × 0.4 mm) were obtained. Space group *P*3121; $a = b = 122.41$, and $c = 111.22$.

Table 2: Crystallographic and Refinement Data

derivative	resolution (Å)	last resolution shell (Å)	no. of measurements (unique)	completeness (in last shell) (%)	R_{merge}[a] (%)	R_{factor} (%)	no. of atoms (total/protein/water)	average temperature factor (Å^2)
DIP	2.53	2.62−2.53	94.914 (29.368)	90.5 (73.0)	11.2		DIP was not further refined	
KPA	2.68	2.78−2.68	79.564 (20.629)	77.6 (79.1)	6.5	18.38	4.643/4.380/241 1	18.85
LPS	2.79	2.89−2.79	76.806 (23.456)	94.0 (68.3)	8.1	19.61	4.647/4.380/221 1	20.90
LYS	2.94	3.04−2.94	59.671 (19.243)	91.5 (77.8)	13.5	19.62	4.640/4.380/238 8	19.03
PHP	2.73	2.78−2.69	57.255 (18.535)	69.1 (65.2)	12.7	18.33	4.624/4.380/232 2	21.24

[a] $R_{merge} = \sum(I_h - |I_h|)/\sum I_h$ for all measurements; I_h is intensity.

(β/α)$_8$-barrel fold with an additional C-terminal domain which is mainly α-helical. Whether this additional domain modulates substrate binding, as has been suggested for the C-terminal domain of type I aldolase and the (β/α)$_8$-barrel enzyme fructose-bisphosphate aldolase (Sygush *et al.*, 1987; Littlechild & Watson, 1993), is not known. The active site lysine (K161; Laber *et al.*, 1992) is located at the C-terminal pole of the barrel structure.

This structural information provided the basis for investigating substrate binding, catalysis, and regulation of DHDPS. Therefore, we studied the three-dimensional structure of *E. coli* DHDPS by X-ray crystallography complexed with (1) pyruvate, (2) the substrate analogs succinate β-semialdehyde (SAS) and α-ketopimelic acid (KPA), (3) the inhibitor dipicolinic acid (DPA), and (4) the natural feedback inhibitor L-lysine. As the product of the reaction catalyzed by DHDPS has not been unequivocally identified, NMR experiments, using ^{13}C-labeled pyruvate as substrate, were conducted. These experiments show that the product released by DHDPS is (4*S*)-4-hydroxy-2,3,4,5-tetrahydro-(2*S*)-dipicolinic acid (HTPA). On the basis of the results obtained by X-ray crystallography and NMR spectroscopy, together with kinetic data, a plausible reaction mechanism is proposed. Second, the lysine effector site is identified, and amino acid side chains important for catalysis and regulation are pointed out.

MATERIALS AND METHODS

Enzyme Purification, Crystallization, and Soaking of Crystals. DHDPS from *E. coli* was purified from an overproducing strain of *E. coli* as described previously (Mirwaldt *et al.*, 1995). Crystals were obtained by the hanging drop method in the presence of β-octyl glucoside using either potassium phosphate buffer (pH 10) or potassium citrate buffer (pH 7.0) as the precipitant (Laber *et al.*, 1992). Crystals of DHDPS complexed with substrate and/or inhibitors were prepared by soaking or cocrystallization under the conditions summarized in Table 1. The crystals were isomorphous with respect to the native crystals.

X-ray Data Collection. The data were collected on a MarResearch image plate scanner (45 kV, 120 mA) mounted on a Rigaku RU200 rotating anode generator (Rigaku, Tokyo, Japan). During data collection, the crystals were cooled to 4 °C by a stream of cold air. The images were processed using the program suite MOSFLM (Leslie, 1990). Scaling and data reduction were performed with ROTAVATA/AGROVATA and TRUNCATE from the CCP4 program suite (CCP4, 1994). Different data sets were scaled with PROTEIN (Steigemann, 1991). After map calculation with PROTEIN, the maps were averaged 2-fold around the local 2-fold axis (Mirwaldt *et al.*, 1995). Rotation and translation matrices, masking of the subunits, and averaging of the electron density maps were performed using MAIN (Turk, 1988). The averaged maps showed a marked improvement with respect to the unaveraged maps. Models of the inhibitors were built into the difference density maps calculated with the $F_o - F_{o'}$ coefficients, where F_o were the observed amplitude of the derivative data set and $F_{o'}$ were the amplitude of the native data set. The phases were derived from the native model. The models of complexes containing the ligand were refined with X-PLOR (Brünger, 1992) using the parameter set of Engh and Huber (1991) to an R_{factor} below 20.0%. The root mean square (rms) of the subunits in the asymmetric unit after refinement was between 0.24 and 0.26 (native model, rms = 0.19). For the inhibitor molecules, strong noncrystallographic symmetry restraints were used. Water molecules not well defined in the electron density or with a B_{factor} of above 50.0 were deleted. Crystallographic and refinement statistics are summarized in Table 2.

Enzyme Assays. DHDPS was assayed as described previously (Laber *et al.*, 1992). For inactivation experiments, DHDPS was preincubated at room temperature in 50 mM Tris-HCl (pH 8.2) with varying concentrations of KPA. At

predetermined time intervals, aliquots were transferred to the standard assay mixture and assayed for enzyme activity.

^{13}C-NMR Spectroscopy. Samples of the enzyme together with the substrates were prepared in a volume of 500 μl, containing 200 mM Tris-HCl (pH 9.0), 50 mM $KHCO_3$, 50 μL of D_2O, 100 mM labeled pyruvate, and 5 μL of DHDPS (2 mg/mL) in Tris-buffer/glycerol. The reaction was initiated by addition of D,L-ASA to a final concentration of 20 mM.

D,L-ASA used for NMR spectroscopy was obtained from Michael Dechantsreiter and was prepared according to the procedure described by Tudor *et al.* (1993).

^{13}C-NMR proton-coupled spectra were started approximately 4 min after addition of ASA. Experiments were performed at 17 °C on a BRUKER AMX 500 MHz spectrometer using a 5 mm triple-resonance probehead. Complex data points (8K) were recorded for each scan with a repetition delay of 2 s. In a pseudo-two-dimensional spectrum, between 50 and 100 single ^{13}C-one-dimensional-experiments were collected. Scans (65, 128, or 256) were acquired for each one-dimensional experiment. This scheme was devised in order to observe the decomposition of the product and obtain optimum signal to noise ratios for signals which are not present during the entire experiment (i.e. signals which either decay or build up). All single experiments of the pseudo-two-dimensional spectrum were Fourier-transformed after apodization with a Gauss window and zero filled to a size of 16K complex data points. A sweep width of 320 ppm was used, and the carrier was placed at 82.5 ppm. The spectra are calibrated using TMS as the external standard. Each spectrum in Figure 5 was obtained by adding the first 50 experiments (64 scans each = a total of 3200 scans) of the pseudo two-dimensional spectrum.

Increment calculations were performed with Spec Tool for Windows, Version 1.1 (Chemical Concepts, 1995).

^{1}H-NMR Spectroscopy. Identical samples were prepared as they were for ^{13}C-NMR spectroscopy, and the reaction was initiated by addition of D,L-ASA. All one- and two-dimensional ^{1}H spectra were recorded at 17 °C on BRUKER AMX 500 and DRX 600 MHzspectrometer. In the one-dimensional ^{1}H spectra, the water resonance was suppressed using a jump−return sequence (Plateau & Gueron, 1982) with the carrier frequency placed on water.

The two-dimensional total correlation spectroscopy (TOCSY) was performed on a BRUKER AMX 500 MHz spectrometer with the MLEV-17 sequence (Bax & Bavis, 1985) for an isotropic mixing time of 36 ms. The double-quantum-filtered correlation spectroscopy (DQF-COSY) (Ernst *et al.*, 1987) was performed on a BRUKER DRX 600 MHz spectrometer in order to distinguish between multiple through-bond-magnetization transfers (as observed in TOCSY) and single-step through bond magnetic transfers (COSY). Both pulse sequences included presaturation of the water resonance (Gueron *et al.*, 1991). The use of different field strengths provides the means for distinguishing between signals originating from two protons giving two signals, which are seperated by a small chemical shift, and from splitting due to *J* coupling. In the TOCSY and DQF-COSY experiments, the carrier was placed at 4.73 ppm for both the direct and indirect dimension. The sweep width was 10 ppm in both dimensions. Complex points (4 K) were acquired in the direct dimension. For the TOCSY 400 increments and for the DQF-COSY 750 increments were recorded. Both spectra were zero filled and Fourier transformed to a final size of 4K × 512 complex points.

RESULTS

Active Site of E. coli DHDPS. Crystallographic studies of native *E. coli* DHDPS had revealed that the active site is a cavity formed by two monomers (Mirwaldt *et al.*, 1995). K161, implicated in Schiff base formation (Laber *et al.*, 1992), is positioned on a hydrophobic scaffold, leaving only one side accessible to the solvent. Y133 is situated close to K161 (3.4 Å) and is part of a hydrogen-bonded triad linking two monomers. Y133 is hydrogen bonded *via* T44 (3.6 Å) to Y107 (2.7 Å) of the neighboring monomer which reaches into the active site. Y107 and Y106 form an aromatic stack with the corresponding residues of the other monomer (Figure 4B). The main chain dihedral angles of Y107 fall into the disallowed region of the Ramachandran plot (Mirwaldt *et al.*, 1995), indicating conformational strain, possibly important for catalysis and/or inhibition. Residues lining the active site are conserved or conservatively exchanged in all DHDPS sequences known to date.

Complex with Pyruvate. To elucidate the first step of the reaction, i.e. Schiff base formation with pyruvate, X-ray data were collected from crystals soaked with pyruvate. The corresponding difference density map showed positive electron density at K161, indicating that Schiff base formation between the ϵ-amino group of K161 and pyruvate had taken place (Figure 2A, atomic distances in Table 3). Identical difference density was obtained from pyruvate/sodium borohydride-inactivated enzyme (Laber *et al.*, 1992), although with lower resolution (data not shown). The carboxyl group of the bound pyruvate is oriented toward Y133 (3.3 Å) and toward T44 and T45 (2.8 Å), which are shifted toward the substrate as compared to the unliganded enzyme. While T44 is linked *via* hydrogen bonds to the adjacent Y133 and to Y107 of the other monomer, T45 is hydrogen bonded to N248 (2.9 Å). N248 is conserved in plants and *E. coli* but replaced by a glycine in Gram-positive bacteria.

Complex with Pyruvate and Succinate β-semialdehyde. Succinate β-semialdehyde (SAS) is an ASA analog in which the amino group has been substituted by a hydrogen atom. SAS is a reversible inhibitor of DHDPS which is competitive with respect to L-ASA (K_i = 0.30 mM) and uncompetitive with respect to pyruvate at nonsaturating L-ASA concentrations. After prolonged incubation of DHDPS with pyruvate and SAS, no pyruvate consumption could be detected.

DHDPS crystals were soaked with pyruvate and SAS both with and without lysine present in the soaking buffer. In both cases, the identical positive difference electron density in the form of a half-circle was observed in the active site (Figures 2B and 3).

Superposition of this density with that obtained from pyruvate soaks showed an overlap at the pyruvate moiety. The overall electron density suggests that SAS has undergone aldol addition to pyruvate. Models of both possible stereoisomers of the aldol adduct were refined into the density; however, only the *S*-isomer was in agreement with the experimental results. The hydroxyl group is within hydrogen-bonding distance to the imine N of K161 (2.8 Å) and to the backbone oxygen of the conserved G186 (2.9 Å). Y133 points toward the center of the half-circle, with a distance

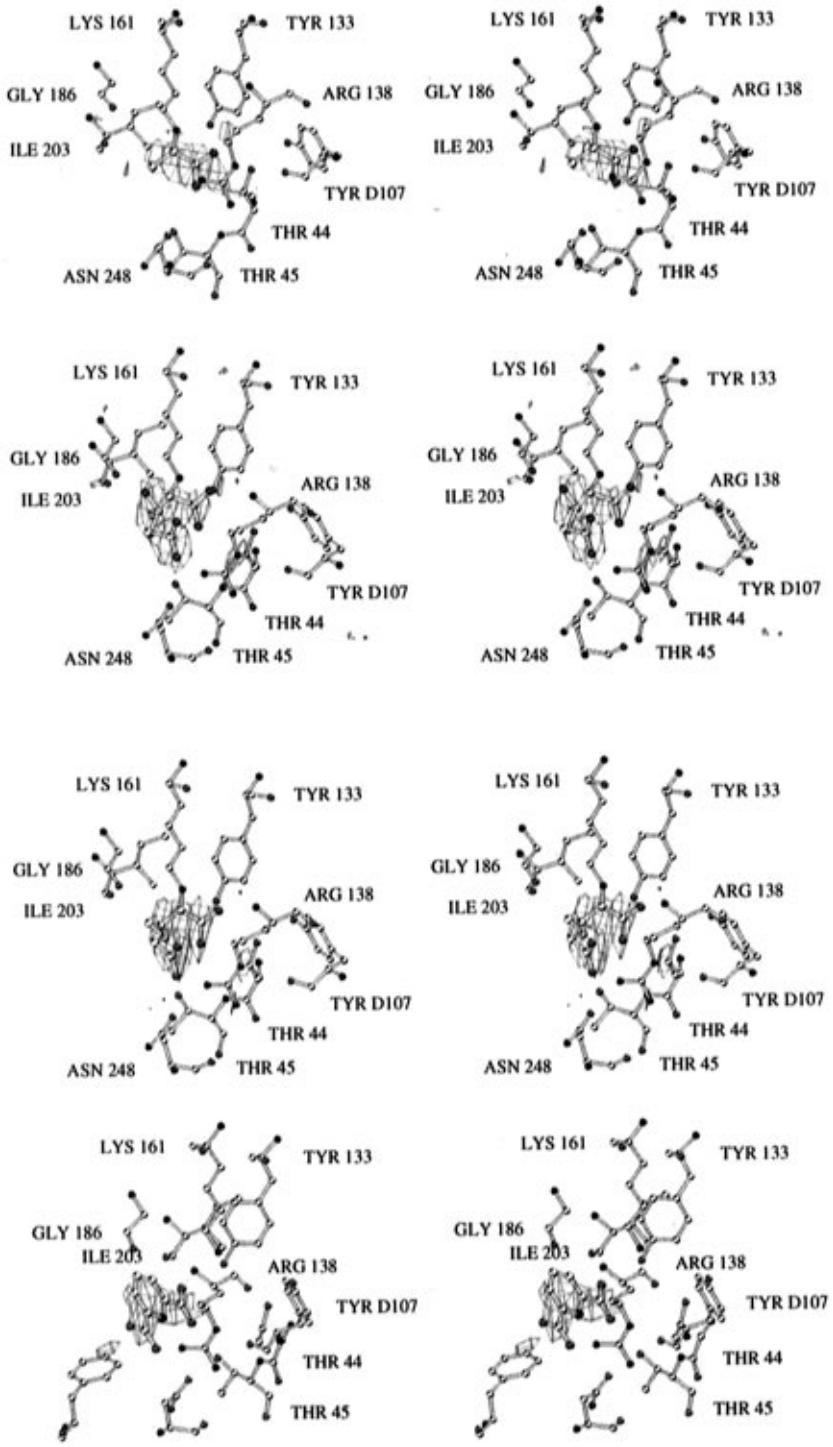

FIGURE 2: Defocused stereoplots of the difference densities in the active site in *E. coli* DHDPS. The plots were made using MOLSCRIPT (Kraulis, 1991) and MINIMAGE (Arnez, 1994). From top to bottom: (A) PHP. Soak with pyruvate, density contoured at 4.7 σ. (B) LPS. Soak with pyruvate, SAS, and lysine, density contoured at 4.5 σ. (C) KPA. Soak with KPA, density contoured at 6.5 σ. (D) DIP. Soak with DPA, density contoured at 5.0 σ.

of approximately 3.3 Å to the hydroxyl group. The aldol adduct is attached to the enzyme through imine formation with K161. Coordination of the carboxyl group of the pyruvate moiety remains unchanged upon addition of SAS, while the second carboxy group is coordinated by the conserved residue R138, which shows positive density, indicating rigidification. Indeed, in the refined model containing the inhibitor, the temperature factors of the side chain of R138 are significantly lowered.

Complex with α*-Ketopimelic Acid.* When DHDPS was preincubated with KPA in the absence of substrates, the enzyme activity decreased as a function of time and inhibitor concentration. Loss of enzyme activity followed pseudo-first-order and saturation kinetics (K_i = 0.17 mM, k_{inact} = 0.77 min^{-1}). Pyruvate protected against loss of enzyme activity, indicating that KPA interacts with the pyruvate binding site. The inhibition of DHDPS by KPA was judged to be irreversible, since gel filtration did not restore the enzyme activity. In the difference electron density map of the enzyme−inhibitor complex obtained after soaking of DHDPS crystals with KPA, positive electron density was found in the active site, corresponding to the bound inhibitor

Table 3: Distances in Native DHDPS and DHDPS Complexed with Bound Pyruvate and SAS of Subunit A

			native (Å)	PHP (pyruvate) (Å)	LPS (lysine/ pyruvate/ SAS) (Å)
protein distances	OH Y133	NT K161	3.4	3.8	4.0
	OH Y133	OH T44	3.6	3.0	2.9
	OH T44	OH Y107	2.7	2.7	2.6
pyruvate	CO1	OH Y133		3.3	3.4
	CO2	OH T45		2.8	3.1
	C2	OH Y133		3.6	3.6
	C3	OH Y133		4.6	4.4
	C3	O I203		3.4	3.6
SAS	CO1	NH_2 R138			3.0
	CO2	NH_2 R138			2.7
	CA	OH Y133			4.7
	OH	O G186			2.9
	OH	OH Y133			3.5
	OH	NT K161			2.8

(Figure 2C). Overlay of the electron density with that obtained from the pyruvate/SAS soaks showed overlap except for the aldol oxygen atom. However, the density of KPA is less well defined, indicating flexibility. Coordination of the two carboxyl groups of KPA is identical to that of the pyruvate−SAS adduct. Again, T44 and T45 are shifted 0.5 Å toward the carboxyl group of the inhibitor.

Complex with Dipicolinic Acid. In order to elucidate the final steps of the reaction, a DHDPS crystal was soaked with dipicolinic acid, a known inhibitor of *E. coli* DHDPS (Couper *et al.*, 1994), which was thought to act as a product analog. Inspection of the corresponding difference map showed positive difference density in the active site (Figure 2D). Dipicolinic acid is coordinated by residues T44, Y133, and R138 and by R109 from the second subunit. Hydrophobic interactions are made with F244, which is situated close to the aromatic ring of the inhibitor and moves slightly toward the inhibitor upon binding. There is no significant overlap with the density obtained from the pyruvate/SAS soak, suggesting that dipicolinic acid does not behave as a product analog. Therefore, the structure of DHDPS with bound dipicolinic acid was not further refined.

Complex with L*-Lysine. E. coli* DHDPS is feedback inhibited by L-lysine with an $I_{0.50}$ of 1 mM (Laber *et al.*, 1992). Our kinetic data show that lysine inhibits DHDPS uncompetitively with respect to pyruvate and noncompetitively with respect to L-ASA. Lysine binding was shown to be cooperative.

To identify the binding site of inhibitory lysine, X-ray data were collected from crystals cocrystallized with lysine and from native crystals soaked with lysine. Identical difference maps were obtained for both experiments. Positive electron density was found at the interface of two monomers (Figures 3 and 4A, atomic distances in Table 4), indicating that two lysine molecules bind around a local 2-fold axis, which rotates one monomer of the dimer onto the other. Each of the two lysines is in contact with both subunits and with each other (distance of the Cα atoms, 4.0 Å). The α-amino group of one inhibitor is 4.4 Å away from the carboxyl group of the second inhibitor and *vice versa*. Thus, the binding pocket of one inhibitory lysine is made up of both dimer-forming monomers and of the adjacent lysine molecule. The side chain of the bound lysine is in a bow-shaped conformation, indicating conformational strain.

The lysine α-amino group is hydrogen bonded to the backbone oxygen of A49 (2.7 Å). The monomers are cross-linked by lysine *via* residues E84 (3.1 Å) and N80 (2.7 Å) of the other subunit. The carboxyl group of the inhibitory lysine is coordinated by the phenolic hydroxyl group of the conserved Y106 (2.6 Å), which is slightly twisted upon inhibitor binding. The lysine ϵ-amino group is coordinated to residues H53 and H56, which are part of helix α2, and through a bridging water molecule, to the backbone oxygen of G78, which is conserved in all known DHDPS sequences.

Upon lysine binding, several residues lining the binding site move to accommodate the inhibitor. H53 shows the most pronounced change, moving 0.6 Å away from the ϵ-amino group of lysine, accompanied by a twist of the ring plane of approximately 70°. This brings H53 to a distance of 3.8 Å from the ϵ-amino group of lysine. H56, which is close to H53, moves toward the lysine ϵ-amino group (4.7 Å). H56 is in the vicinity of E84 of helix α3 of the same subunit (3.3 Å). E84 moves toward H56 and forms a salt bridge with the α-amino group of the inhibitory lysine of the other monomer (3.1 Å). The combined movement of H53 and H56 induces a movement of helix α2 toward the lysine binding site. The helix lies well away from the active site and does not take part in any contacts between the monomers. No other significant movements of the enzyme could be discerned.

^{13}C-NMR Studies Using Labeled Pyruvate. Due to its instability, the product of the reaction catalyzed by DHDPS has never been unequivocally identified. Indirect evidence has been put forward indicating that 2,3-DHDP is formed in the course of the reaction (Yugari & Gilvarg, 1965). However, the formation of HTPA, 2,5-DHDP, or even a mixture of these together with the respective open chain isomers could not be excluded (Shedlarski & Gilvarg, 1969). Accordingly, upon synthesis of THDP, a complex mixture of products including the open chain isomer was found (Couper & Robins, 1992). Therefore, NMR experiments were conducted, using [3-^{13}C]pyruvate and [2,3-^{13}C]pyruvate as a substrate for *E. coli* DHDPS. The reaction was initiated in the NMR tube by addition of D,L-ASA, and the progress of the reaction was monitored by ^{13}C-NMR (Figure 5). Two product signals were identified using doubly labeled pyruvate: a triplet (J_{CH} = 132.9 Hz) of doublets (J_{CC} = 36.5 Hz) at 34 ppm and a doublet (J_{CH} = 36.5 Hz) at 166.5 ppm. Using [3-^{13}C]pyruvate only, a triplet at 34 ppm developed (J_{CH} = 132.9 Hz). The doublet at 166.5 ppm was assigned to C2 of the pyruvate moiety and is interpreted to arise from the formation of a cyclic imine, as increment calculations firmly place the signal of an open chain isomer above 180 ppm (the chemical shift of the C2 of pyruvate is 203.5 ppm). The signal at 34 ppm was assigned to C5 of the cyclic product, indicating the formation of a methylene group originating from C3 of pyruvate. Performing the reaction at physiological pH produced identical signals, which however rapidly decomposed together with intense coloring of the solution, in strong contrast to the stability of the product at pH 9.0.

^{1}H-NMR Studies Using Labeled Pyruvate. From the ^{13}C-NMR experiments. it can be concluded that DHDPS catalyzes the condensation of pyruvate and L-ASA to a cyclic product through imine formation. Second, the obtained

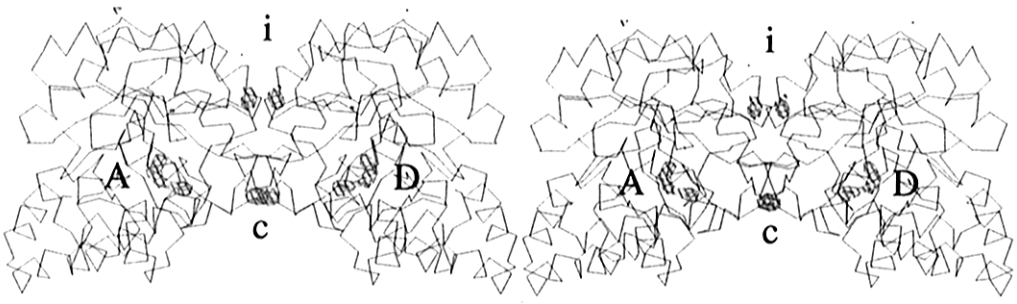

FIGURE 3: LPS. Defocused stereoplot of difference density covering a dimer of *E. coli* DHDPS soaked with pyruvate, SAS, and lysine, density contoured at 5.5σ. The plots was made using MOLSCRIPT (Kraulis, 1991) and MINIMAGE (Arnez, 1994): i, binding site of inhibitory lysine; and A and D, active sites of the dimer; and c, movement of C141.

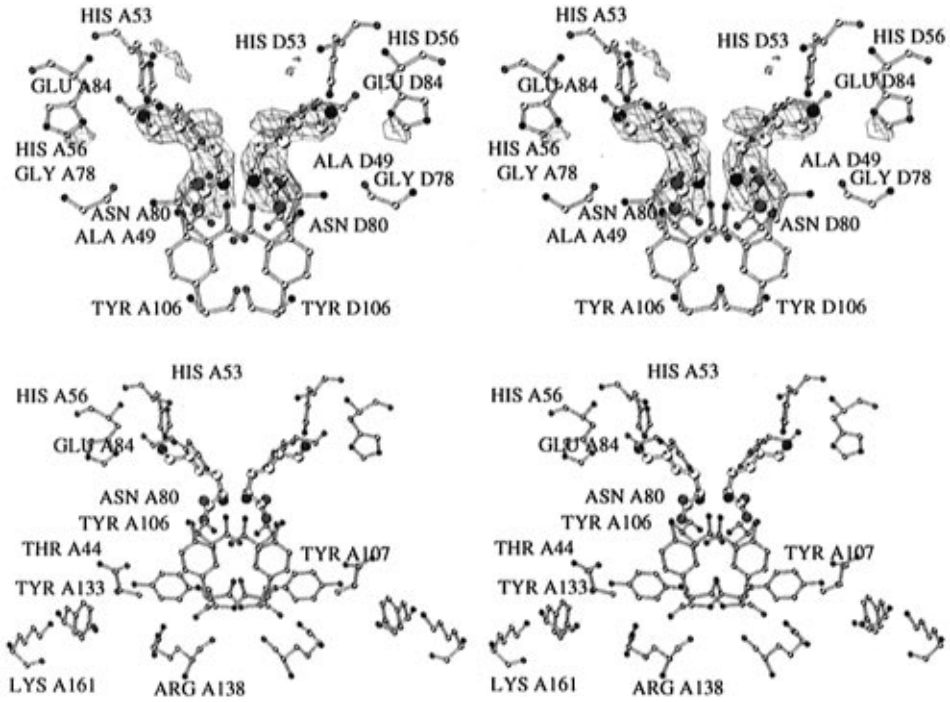

FIGURE 4: Inhibitor binding site and connection to the active site.The plots were made using MOLSCRIPT (Kraulis, 1991) and MINIMAGE (Arnez, 1994). (A, top) LYS. Defocused stereoplot of difference density at the inhibitor binding site, density contoured at 5.5σ. Defocused stereoplot showing the positions of the inhibitory lysines relative to the active site lysine K161. For clarity, only the residues of subunit A were labeled.

Table 4: Distances of Coordinating Residues to L-Lysine

	residue	distance (Å)	comment
OC1	OH Y106	2.6	slight movement upon inhibitor binding
Nα	O A49	2.7	no movement
Nα	NH_2 N80	3.9	no movement
Nα	O N80	2.7	cross-linking of monomers *via* binding of the inhibitor
Nα	O E84	3.1	cross-linking of monomers *via* binding of the inhibitor
Nϵ	NH H53	4.7	reorientation upon inhibitor binding
Nϵ	NH H56	3.8	reorientation upon inhibitor binding
Nϵ	H_2O	2.6	H_2O coordinated by O G78 (2.9 Å)

spectra show that C5 is not involved in a possible elimination of the hydroxy group and double-bond formation. Therefore, 2,3-DHDP is not the immediate product of the reaction catalyzed by DHDPS. In order to distinguish between the possible products 2,5-DHDP and HTPA, one-dimensional and two-dimensional ^{1}H-NMR studies were conducted. The starting point was the identification of a doublet in the one-dimensional ^{1}H-NMR at 2.8 ppm, which was split into a double doublet (J_{CH} = 132.9 Hz) when using [3-^{13}C]pyruvate (Figure 6a). The signal was assigned to the axial proton at C5 of the product (^{a}H in Figure 7). Doublet formation is due to geminal coupling to the equatorial proton (^{e}H in Figure 7) at C5 (18 Hz). The corresponding signal of ^{e}H (2.0 ppm) was identified by comparison of a COSY spectrum recorded using unlabeled pyruvate with a TOCSY spectrum recorded using [3-^{13}C]pyruvate (Figure 6b,c). It also showed the characteristic splitting due to C−H coupling. Assignment of axial and equatorial positions was on the basis of vicinal coupling of ^{a}H to an axial proton at C4 (6 Hz). The chemical shift of 3.9 ppm for the proton at C4 (Figure 6b,c) is consistent with HTPA as the product of DHDPS. No signal above 4.1 ppm hinting at double-bond formation could be detected. Together with the observation of a signal at 1.28 ppm (Figure 6b), which was assigned to C3 of HTPA, formation of 2,5-DHDP can therefore be excluded. On the basis of the cross-coupling peaks in the TOCSY spectrum, the methylene group C3 is assigned to a signal at 1.3 ppm and the chiral proton at C2 assigned to 4.0 ppm.

The product is released from the enzyme without elimination of water and double-bond formation; therefore,

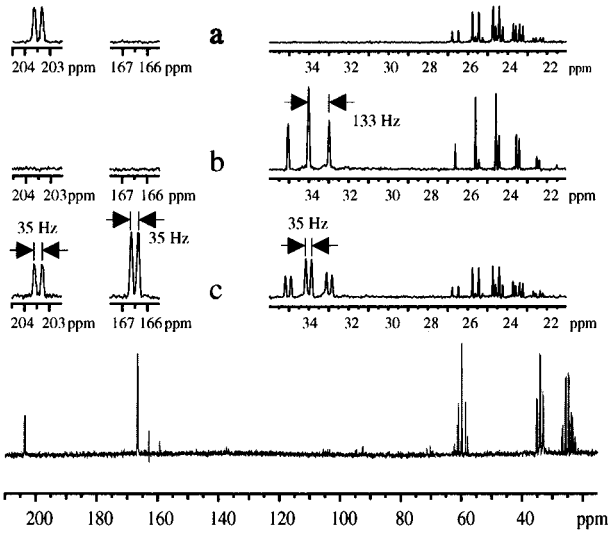

FIGURE 5: 125 MHz spectrum of *E. coli* DHDPS after completion of the reaction of [2,3-^{13}C]pyruvate with ASA. Signals of pyruvate and its hydrate at 25 and 203 ppm; product signals at 34 and 166.5 ppm. Signals at 60 ppm are from the buffer system used. (a) Details of the reference spectrum with [2,3-^{13}C]pyruvate and DHDPS and without addition of ASA. (b) Details of the spectrum of *E.coli* DHDPS after completion of the reaction of [3-^{13}C]pyruvate with ASA. (c) Details of the spectrum of *E. coli* DHDPS after completion of the reaction of [2,3-^{13}C]pyruvate with ASA.

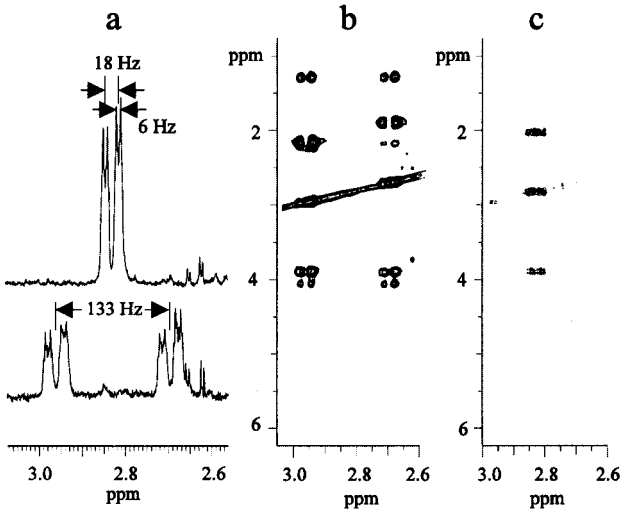

FIGURE 6: ^{1}H-NMR spectroscopy. Spectra taken with unlabeled pyruvate were recorded on a 600 MHz spectrometer, and spectra taken with ^{13}C-pyruvate were recorded on a 500 MHz spectrometer to distinguish between signals originating from two protons giving two signals, which are seperated by a small chemical shift, and from splitting due to *J* coupling. (a) Details of one-dimensional ^{1}H-NMR spectra showing the ^{13}C splitting of the signal of the axial proton ^{a}H of HTPA. The spectrum of the unlabeled sample was taken on a 600 MHz spectrometer and the spectrum of the sample containing the [3-^{13}C]pyruvate on a 500 MHz spectrometer. (b) Strip of a TOCSY spectrum showing connectivities from the axial proton ^{a}H of HTPA. Visible are cross-peaks due to a geminal coupling constant to ^{e}H (1.90 and 2.18 ppm), a vicinal coupling constant to the proton at C4 (3.9 ppm), and a ^{4}J-coupling to the methylene protons at C3 (1.28 ppm) and to the chiral proton at C2 (4.0 ppm). Note the splitting of the signals due to the presence of ^{13}C in position C5 of HTPA. (C) Strip of a COSY spectrum taken with unlabeled pyruvate, showing spin−spin coupling of the axial proton ^{a}H with adjacent protons. A cross-peak due to geminal coupling to the equatorial proton ^{e}H (2.0 ppm) and a cross-peak originating from vicinal coupling to the proton at C4 (3.9 ppm) are visible.

2,3-DHDP is not the immediate product of the reaction catalyzed by DHDPS. On the basis of these results, it is concluded that DHDPS catalyzes the reaction of pyruvate with L-ASA to form HTPA.

DISCUSSION

Proposed Reaction Mechanism. The reaction catalyzed by DHDPS can be divided into three consecutive steps: Schiff base formation with pyruvate, followed by addition of L-ASA, and finally transimination leading to cyclization with simultaneous dissociation of HTPA (Figure 7).

Schiff Base Formation. The reaction is initiated by a nucleophilic attack of the ϵ-amino group of K161 to the keto group of pyruvate, resulting in the formation of the imine. Although there are no experimental data currently available, K161 is proposed to be in a nonionized state prior to substrate binding, as has been demonstrated for fructose-1,6-bisphosphate aldolase, which catalyzes a highly similar retro aldol reaction; fructose 1,6-bisphosphate is cleaved to dihydroxyacetone phosphate and glyceraldehyde 3-phosphate *via* an enamine/carbanion mechanism. Here the active site lysine was found to be unprotonated at physiological pH in the absence of substrate (Healy & Christen, 1973; Morris & Tolan, 1994). A tyrosine residue of the C terminus has been proposed to act as both the proton donator and acceptor during the Schiff base formation preceding the cleavage of the carbon−carbon bond (Littlechild & Watson, 1993).

Formation of the Schiff base proceeds through a tetrahedral transition state (Figure 7, step I). The proximity of C2 of the bound pyruvate to the phenolic hydroxy group of Y133 (3.4 Å) suggests that Y133 assists the reaction through a hydrogen bond to the keto oxygen of pyruvate. An identical role has been suggested for Y152 in 3α(or 20β)-hydroxysteroid dehydrogenase, which catalyzes the inactivation of circulating steroid hormones. Y152 acts as a general acid, protonating the acceptor carbonyl and facilitating the nucleophilic attack of the hydride ion (Jörnvall *et al.*, 1995). Similarly, a tyrosine residue (Y7) enhances the nucleophilicity of a thiol group in glutathione *S*-transferases (Reinemer *et al.*, 1991).

Aldol Reaction. L-ASA adds with its aldehyde group to the enamine of the Schiff base (step III). Tautomerization of the Schiff base was demonstrated to proceed in the absence of L-ASA, as exchange with the solvent was observed upon addition of DHDPS to 3-^{3}H-labeled pyruvate (Shedlarski & Gilvarg, 1969). Interestingly, the pH optimum for the exchange reaction, interpreted as enamine formation, was slightly acidic as compared to the overall optimum for the reaction catalyzed by DHDPS of pH 8.4. In type I aldolases, proton transfer leading to enamine formation may be mediated either by a water molecule or a tyrosine residue (Littlechild & Watson, 1993). In *E. coli* DHDPS, the distance of the phenolic hydroxy group of Y133 to C3 of the bound pyruvate (>4 Å) makes a catalytic role for Y133 in enamine formation unlikely. Whether the backbone oxygen of I203 (approximately 3.5 Å to C3), which is conserved or conservatively exchanged in DHDPS isoenzymes, plays an additional role in enamine formation is unclear.

It has recently been observed that the hydrate of ASA is the predominant species in aqueous solution (Tudor *et al.*, 1993; Coulter *et al.*, 1996). As the active site of DHDPS is spatially able to accommodate the hydrate, and G186 and

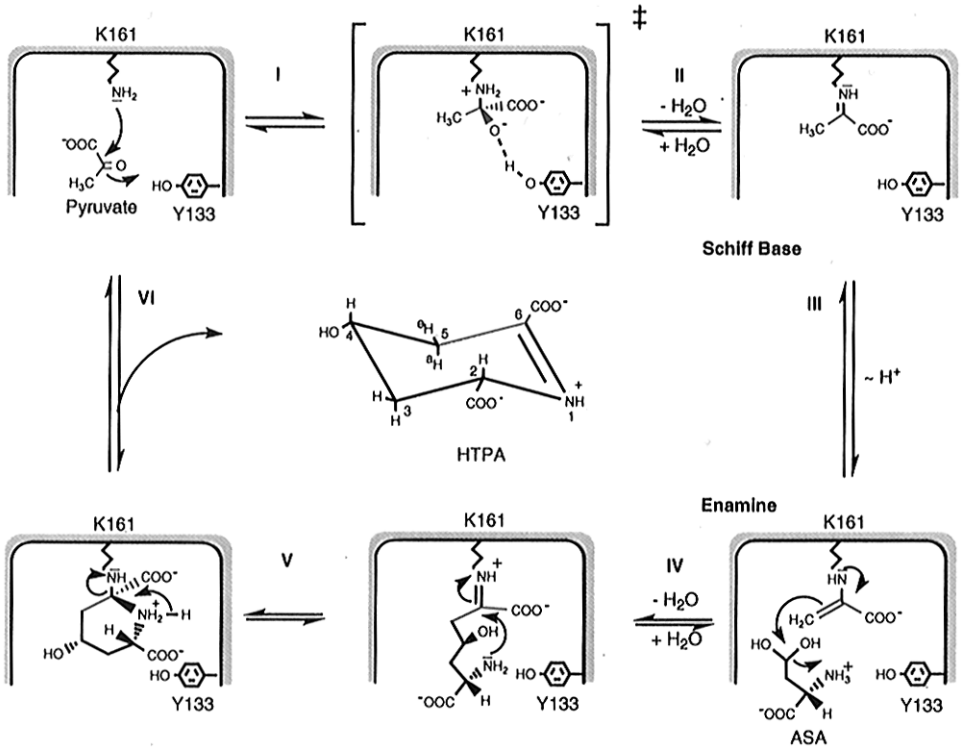

FIGURE 7: Proposed reaction mechanism of DHDPS.

N248 are in favorable position to coordinate the hydroxyl groups, it is proposed that the hydrate of L-ASA is bound to the active site of DHDPS prior to the aldol reaction.

Nucleophilic attack of the enamine to the hydrate of L-ASA leads to formation of the new C−C bond with displacement of a water molecule (step IV). The orientation of the resulting complex is proposed to be similar to the complex of the ASA analog SAS bound to pyruvate (Figure 2B).

Transimination and Formation of 4-Hydroxy-2,3,4,5-tetrahydrodipicolinic Acid. Our experiments using ^{13}C-labeled pyruvate support the view that the product released from DHDPS is HTPA and not 2,3-DHDP, as previously assumed. The release of the open chain isomer and cyclization in solution are unlikely because no corresponding peaks accumulate according to NMR spectroscopy. This interpretation is supported by the observation that hydrolysis of the Schiff base after the aldol reaction of SAS with the enzme-bound enamine of pyruvate is not possible, as no consumption of pyruvate and no product signal in ^{13}C-NMR could be detected upon addition of SAS. Furthermore, KPA acts as an irreversible inhibitor of *E. coli* DHDPS, presumably because KPA covalently bound to DHDPS lacks the hydroxyl group necessary for reverse aldol reaction, and as hydrolysis of the Schiff base is not possible, the enzyme is effectively inactivated. It is therefore proposed that the presence of the second carboxyl group in the active site modulates the reactivity of the Schiff base to ensure transimination. Titration of the active site of aspartate amino transferase showed an analogous effect, with the pK_a of the imine rising approximately 2 units upon substrate binding (Yano *et al.*, 1993). The pK_a shift upon substrate binding is suggested to be caused by compensation of the positive charge resulting from protonation of the aldimine by the carboxylate groups of the substrate and through changes in the electrostatic environment of the active site.

For the final steps of the reaction, deprotonation of the attacking amino group and transfer of a proton to the ϵ-amino group of K161 are necessary. Y133 is proposed to play a central role in these steps, as it is in position to coordinate the attacking amino group both before and after nucleophilic attack. Transfer of protons is possible to the ϵ-amino group of K161 *via* the hydroxyl group of the aldol complex and to the solvent *via* T44 and Y107. A similar proton shuttle has been proposed in pyridoxal phosphate (PLP)-containing enzymes (Weng & Leussing, 1983). The phenolic oxygen of PLP transfers protons from the nitrogen of the reactant to the nitrogen of lysine, transferring as many as three protons from the attacking ammonium cation.

HTPA is thus formed by nucleophilic attack of the amino group of L-ASA to the Schiff base (step V), leading to cyclization and the stepwise detachment (step VI) of the product from the enzyme.

The stereochemistry at C4 of HTPA is deduced from the observation that SAS binds to the enzyme-bound enamine of pyruvate to form a complex in which the new stereocenter at the carbon, maintaining the hydroxy group, has an *S* configuration (Figure 2B). Together with the signals obtained by one-diemsional ^{1}H-NMR, which show that only one product is formed, it is concluded that racemization in solution *via* double-bond formation does not take place.

Whether DHDP is subsequently formed under physiological conditions remains to be elucidated. Although no corresponding signals could be found by ^{13}C-NMR, this may be due to the high pH of the sample. The observed rapid decomposition of the ^{13}C-NMR signals of HTPA at pH 7 indicates that formation of DHDPS at physiological pH may occur in a nonenzymatic step in solution.

Feedback Inhibition. The difference map of DHDPS soaked with its feedback inhibitor reveals that the lysine binding site is located at the monomer−monomer interface. The effector binding site for each lysine molecule is made

up by both dimer-forming monomers and the lysine molecule bound to the neighboring monomer. The architecture of the effector binding site may explain the cooperativity of inhibitor binding, which was observed in the kinetic experiments. As each lysine molecule is part of the coordination sphere of the second lysine (Figure 4A), the affinity of the second lysine molecule to the binding site is increased after the first lysine has been bound. The residues responsible for coordination of the carboxyl and the α-amino group of the effector are highly conserved in all DHDPS sequences known to date. The only exception is E84, which is changed to either T or D in Gram-positive bacteria insensitive to feedback inhibition. Mutations of E84 in maize (Shaver *et al.*, 1996) and of N80 in tobacco DHDPS (Ghislain *et al.*, 1995), both involved in coordination of lysine, confer insensitivity to lysine inhibition, thereby emphasizing the importance of these residues for lysine coordination and/or inhibition.

Residues responsible for coordination of the lysine ϵ-amino group, however, vary strongly in various DHDPS enzymes sensitive to lysine inhibition. This variability, together with the conformational strain generated by the bow-shaped conformation of the side chain of the bound lysine, suggests that this part of the binding site is responsible for modulation of the binding affinity of lysine. Although several residues of the inhibitor binding site are reoriented upon lysine binding, no pathway conveying inhibition to the active site can be identified yet. On the basis of our data, however, some residues important to inhibition can be identified.

(i) Y106 and Y107, which are conserved in all DHDPS enzymes, form a hydrophobic stack with the corresponding residues from the other dimer-forming monomer. This stack connects the inhibitor binding site with both active sites of the dimer (Figure 4B). Y106 and Y107 are assumed to be involved both in lysine inhibition, *via* coordination of the lysine carboxy group by Y106, and in catalysis, as Y107 is connected *via* T44 to Y133 of the active site. Y133 is important for Schiff base formation and subsequent reaction steps leading to product formation. Lysine binding may therefore modulate the catalytic function of Y133.

(ii) R138 is responsible for coordination of the carboxyl group of L-ASA, as demonstrated by the structure of LPS and KPA (Figure 2b,c). Nucleophilic attack of the α-amino group of L-ASA on the Schiff base with K161, a prerequisite for product formation, requires contraction of the reaction intermediate, which in turn induces a movement of R138 in step V of Figure 7. After binding to the regulatory site, lysine is connected to R138 *via* N80 and Y107. Mutation of N80 to Ile renders tobacco DHDPS insensitive to lysine inhibition. It is therefore suggested that feedback inhibition of DHDPS by lysine is, at least partly, accomplished through reduction of the flexibility of R138. This model of inhibition is in accordance with the kinetic data, which show that L-lysine is a noncompetitive inhibitor of DHDPS with respect to L-ASA.

Comparison to N-Acetylneuraminate Lyase. DHDPS displays significant sequence homology with respect to *N*-acetylneuraminate lyase (Neu5Ac) of *E. coli*, a $(\beta/\alpha)_8$-barrel enzyme catalyzing the cleavage of *N*-acetylneuraminic acid to pyruvate and *N*-acetylmannosamine (Izard *et al.*, 1994). The reaction mechanism of Neu5Ac is proposed to proceed *via* Schiff base formation with an active site lysine, followed by a retro aldol reaction. Active site residues of *E. coli* DHDPS T44, T45, Y133, K161, G186, Y107, and I203 are conserved in *N*-acetylneuraminate lyase (EC 4.1.3.3), while Y106 has been exchanged to phenylalanine. When both structures are aligned (coordinates of Neu5Ac were obtained from the Protein Data Bank), we found that these residues have the same spatial positioning. The mechanism of Schiff base formation and the subsequent aldol reaction therefore are likely to be conserved in both enzymes.

ACKNOWLEDGMENT

We thank Dr. Christian Mirwaldt for his support, Dr. Ingo Korndörfer for stimulating discussions, and Dr. Sabine Rudolph-Böhner and Dr. Michael Czisch for their help with NMR spectroscopy.

REFERENCES

Arnez, J. G. (1994) *J. Appl. Crystallogr. 27*, 649−653.
Bakhiet, N., Forney, F. W., Stahly, D. P., & Daniels, L. (1984) *Curr. Microbiol. 10*, 195−198.
Bartlett, A. T. M., & White, P. J. (1986) *J. Gen. Microbiol. 132*, 3169−3177.
Brünger, A. (1992) *X-PLOR (Version 3.1) Manual*, Yale University Press, New Haven and London.
CCP4 (1994) *Acta Crystallogr., Sect. D 50*, 760−763.
Coulter, C. V., Gerrard, J. A., Kraunsoe, J. A. E., Moore, D. J. & Pratt, A. T. (1996) *Tetrahedron 52*, 7127−7136.
Couper, L., & Robins, D. J. (1992) *Tetrahedron Lett. 33*, 2717−2720.
Couper, L., Mckendrick, J. E., Robins, D. J., & Chrystal, E. J. T. (1994) *Bioorg. Med. Chem. Lett. 4*, 2267−2272.
Cremer, J., Treptow, C., Eggeling, L., & Sahm, H. (1988) *J. Gen. Microbiol. 134*, 3221−3229.
Davies, D. G., & Bax, A. (1985) *J. Am. Chem. Soc. 107*, 2820−2821.
Dereppe, C., Bold, G., Ghisalba, O., Ebert, E., & Schär, H.-P. (1992) *Plant Physiol. 98*, 813−821.
Engh, R. A., & Huber, R. (1991) *Acta Crystallogr., Sect. A 98*, 392−400.
Ernst, R. R., Bodenhausen, G., & Wokaun, A. (1987) *Principles of NMR in one and two dimension*, Clarendon Press, Oxford.
Frisch, D. A., Gengenbach, B. G., Tommey, A. M., Sellner, J. M., Somers, D. A., & Myers, D. E. (1991) *Plant Physiol. 96*, 444−452.
Ghislain, M., Frankard, V., & Jacobs, M. (1990) *Planta 180*, 480−486.
Ghislain, M., Frankard, V., & Jacobs, M. (1995) *Plant J. 8*, 733−743.
Grazi, E., Cheng, T., & Horecker, B. L. (1962) *Biochem. Biophys. Res. Commun. 7*, 250−253.
Gueron, M., Plateau, P., & Decorps, M. (1991) *Prog. Nucl. Magn. Reson. Spectrosc. 23*, 135−209.
Healy, M. J., & Christen, P. (1973) *Biochemistry 12*, 35−41.
Hoganson, D. A., & Stahly, D. P. (1975) *J. Bacteriol. 124*, 1344−1350.
Izard, T., Lawrence, M. C., Malby, R. L., Lilley, G. G., & Colman, P. M. (1994) *Structure 2*, 361−369.
Jörnvall, H., Perrson, B., Krook, M., Atrian, S., González-Duarte, R., Jeffery, J., & Ghosh, D. (1995) *Biochemistry 34*, 6003−6013.
Kraulis, P. J. (1991) *J. Appl. Crystallogr. 24*, 946−950.
Kumpaisal, R., Hashimoto, T., & Yamada, Y. (1987) *Plant Physiol. 85*, 145−151.
Laber, B., Gomis-Rüth, X., Romão, M. J., & Huber, R. (1992) *Biochem. J. 288*, 291−295.
Leslie, A. G. W. (1990) in: *Crystallographic computing*, Oxford University Press, New York.
Littlechild, J., & Watson, H. C. (1993) *Trends Biochem. Sci. 18*, 36−39.
Mirwaldt, C., Korndörfer, I., & Huber, R. (1995) *J. Mol. Biol. 246*, 227−239.
Morris, A. J., & Tolan, D. R. (1994) *Biochemistry 33*, 12291−12297.
Plateau, P., & Gueron, M. (1982) *J. Am. Chem. Soc. 104*, 7310−7311.

Reinemer, P., Dirr, H. W., Ladenstein, R., Schäffer, J., Gallay, O., & Huber, R. (1991) *EMBO J. 10*, 1997−2005.
Selli, A., Crociani, F., Di Gioia, D., Fava, F., Crisetig, G., & Matteuzi, D. (1994) *Ital. J. Biochem. 4*, 29−35.
Shaver, J. M., Bittel, D. C., Sellner, J. M., Frisch, D. A., Somers, D. A., & Gengenbach, B. (1996) *Proc. Natl. Acad. Sci. U.S.A. 93*, 1962−1966.
Shedlarski, J. G., & Gilvarg, C. (1969) *J. Biol. Chem. 245*, 1362−1373.
Stahly, D. P. (1969) *Biochim. Biophys. Acta 191*, 439−451.
Steigemann, W. (1991) *Crystallographic computing 5*, Oxford University Press, Oxford.
Sygush, J., Beaudry, D., & Allaire, M. (1987) *Proc. Natl. Acad. Sci. U.S.A. 84*, 7846−7850.
Tosaka, O., & Takinami, K. (1978) *Agric. Biol. Chem. 42*, 95−100.
Tudor, D. W., Lewis, T., & Robins, D. J. (1993) *Synthesis*, 1061−1062.
Turk, D. (1988) *Development and usage of a molecular graphics program*, Ph.D. Thesis, University in Ljubljana, Slovenia.
Wallsgrove, R. M., & Mazelis, M. (1981) *Phytochemistry 20*, 2651−2655.
Webster, F. H., & Lechowich, R. V. (1970) *J. Bacteriol. 101*, 118−126.
Weng, S. H., & Leussing, D. L. (1983) *J. Am. Chem. Soc. 105*, 4082−4090.
Yakamura, F., Ikeda, Y., Kimura, K, & Sasakawa, T. (1974) *J. Biochem. 76*, 611−621.
Yano, T., Mizuno, T., & Kagamiyama, H. (1993) *Biochemistry 32*, 1810−1815.
Yugari, Y., & Gilvarg, C. (1965) *J. Biol. Chem. 240*, 4710−4716.

BI962272D